

## F/48 Slit Spectroscopy

R. Jedrzejewski & M. Voit

*Space Telescope Science Institute, Baltimore, MD 21218*

**Abstract.** The calibration of the FOC F/48 long-slit spectrograph is described. The time-varying and nonlinear geometric distortion makes both target acquisition and spectral rectification difficult. Here we describe the methods developed to ensure adequate calibration accuracy, and present our best understanding of the precision achievable with this instrument.

### 1. Introduction

The F/48 long-slit spectrograph was designed to allow spatially resolved spectroscopy of extended, high surface brightness objects at a wavelength resolution that provides accuracies of tens of km/s or so. However, the difficulties of accurately locating the narrow ( $0''.1$  pre-COSTAR) slit and the subsequent problems of the F/48 detector experiencing a coronal discharge and tripping its high voltage power supply meant that this powerful facility saw little use before the First HST Servicing Mission in 1993. The installation of COSTAR made the slit even narrower ( $0''.062$ ), and at the time of the Servicing Mission it was not clear what the long-term prospects for reliability of the F/48 camera were. However, cautious attempts to use the relay were initially successful, so work was started to try and locate the spectrograph slit and characterize the properties of the spectrograph in order to enable a science program of FOC IDT observations, and to allow GO use in Cycle 6 at the proposer's risk. Despite the fact that the F/48 longslit spectrograph introduced a unique facility to the observatory, only one Cycle 6 GO proposal was accepted. The FOC IDT reserved a significant amount of its guaranteed time for spectroscopic observations, giving a total usage of about 40 orbits.

### 2. F/48 Spectrograph Characteristics

The main characteristics of the F/48 spectrograph are given in Table 1. In all respects (sensitivity, choice of gratings and slits), STIS is a superior instrument, but the F/48 spectrograph had the unique position of being the only long-slit spectrograph on HST before the Second Servicing Mission.

### 3. Calibration

In order to enable the science program, it is necessary to locate the slit on the OTA focal plane or else generate a robust method of acquiring targets onto the slit. Then a first order characterization is necessary to ensure that the performance is close to expectations, so that the science data has the signal-to-noise ratio and other characteristics assumed by the proposers.

Table 1. Characteristics of the F/48 Spectrograph

Slit length:	12.5"
Slit width:	0.062"
Wavelength range:	3600–5400Å first order 1800–2700Å second order 1200–1800Å third order 1150–1350Å fourth order
Dispersion:	1.7 Å/pixel first order
Wavelength resolution:	3 pixels FWHM = 5.1Å = ~400 km/s @ 3727Å
Spatial resolution:	2–3 pixels = 0'05–0'08
Detector Background:	~ 0.3–1 × 10 <sup>-2</sup> counts/pixel/sec
Sensitivity:	$B = 14.6$ mag ⇒ ~ 0.3 count/sec peak @ 4200Å ~ 1 count/sec total @ 4200Å

### 3.1. Slit location

The design of the spectrograph does not make target acquisition easy. The slit is etched into the F/48 aperture plate, offset from the central clear imaging aperture. Light that passes through the slit normally misses the detector. However, when the spectrograph mirror is inserted, the direct light is blocked out and the light through the slit is directed onto a grating, where it is dispersed and fed back onto the detector. The only clue as to the location of the slit is the slit finger, a small opaque protrusion that blocks some direct light at the edge of the F/48 512×1024(z) field of view. Once the shadow of the slit finger is known, in principle the slit can be located provided that one knows the angle that the aperture plate makes with the (V2, V3) system. Unfortunately, the geometric distortion is quite severe at the edge of the field where the image of the slit finger is, so that the slit finger appears to be bent, and this uncertainty in the orientation of the slit finger translates into a large (~ 1" or so) uncertainty in the location of the slit.

Early attempts to locate the slit involved scanning an astrometric standard star over the slit finger (to locate the (V2, V3) coordinates of the finger), and then scanning an astrometric star across the slit. Unfortunately, successive scans failed to give a consistent answer to the location of the slit.

After COSTAR was installed (and the focal plane metrology changed too!), a different method was used. It was realized that it is not necessary to know the absolute location of the slit in (V2, V3) space, only the offset from a reference point in the imaging field. Choosing the reference point to be close to the center of the field, where the changes in geometric distortion are small, should provide some insurance against changes in the distortion that acquisitions in the area close to the slit finger would have been prone to. The offset was determined by scanning a complex target (the AGN NGC 4151) across the slit, and comparing the structure of spectrum of the narrow-line region with narrow-band images taken with the F/96 camera. Having located the offset of the slit, the Project Data Base Science Instrument Aperture File was updated to reflect this knowledge.

But there remains the problem of being able to reliably acquire targets onto the slit. There is no onboard target acquisition facility in the F/48 camera. Actually, that's not quite true. There *is* an onboard target acquisition facility, but the acquisition aperture (63 × 63 pixels) is so small (1"8), that it would require an interactive acquisition to reliably place a target in the acquisition aperture. So it is necessary to use an interactive target acquisition (a so-called "Mode-1 Target Acquisition").

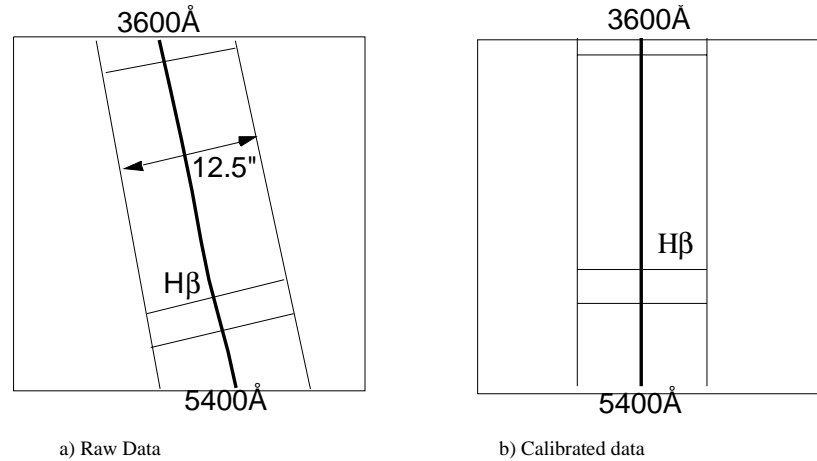


Figure 1. Geometric Distortion in Spectrograph Data

Unfortunately, the geometric distortion is quite nonlinear. This means that the OPUS target acquisition software, which uses a linear distortion model, is not accurate enough to calculate the offset required to move a target to the reference point; the error from using a linear approximation to the distortion can amount to many pixels, or rather larger than the width of the slit.

To overcome this, the geometric distortion of the F/48 imaging camera was measured in the same way as was done for the F/96 camera, by observing a crowded field with multiple pointings. This gives us a detailed model of the geometric distortion stored as a bicubic spline, and an IDL procedure was written to use this spline to calculate the slew required to move the target from the position in the acquisition image to the slit acquisition reference point. This procedure is now routinely used instead of the standard OPUS target acquisition software for interactive acquisitions onto the F/48 slit, and occasionally for F/96 interactive acquisitions when very accurate pointing is required.

Typically, the accuracy of this acquisition method is slightly better than the width of the slit; the main source of residual error is the fact that the geometric distortion is time dependent, so the pixel location of the slit acquisition reference point changes slightly from program to program. A slight improvement can be obtained by scanning the target across the slit, but this is expensive in terms of telescope time.

More details about the procedure for acquiring targets onto the F/48 slit can be found in FOC Instrument Science Report FOC-095.

#### 4. Wavelength Calibration and Rectification

The geometric distortion of the F/48 camera makes analysis of the longslit spectroscopic data difficult. Both the wavelength and the position along the slit are complex functions of pixel location, whereas “calibrated” data would have wavelength a linear function of pixel location in one dimension, and position along the slit a linear function of pixel location in the perpendicular direction. This is exemplified in Figure 1. The F/48 spectrograph does not have an internal emission-line source which could be used for wavelength calibration and wavelength rectification. Nor does it come with a slit mask, which would be useful for determination of the paths traced by point continuum sources. Instead, celestial targets must be used for this type of calibration.

For the wavelength calibration, the high surface brightness planetary nebula NGC 6543 was used. This has many strong first-order lines and fills the spectrograph slit. Using tasks

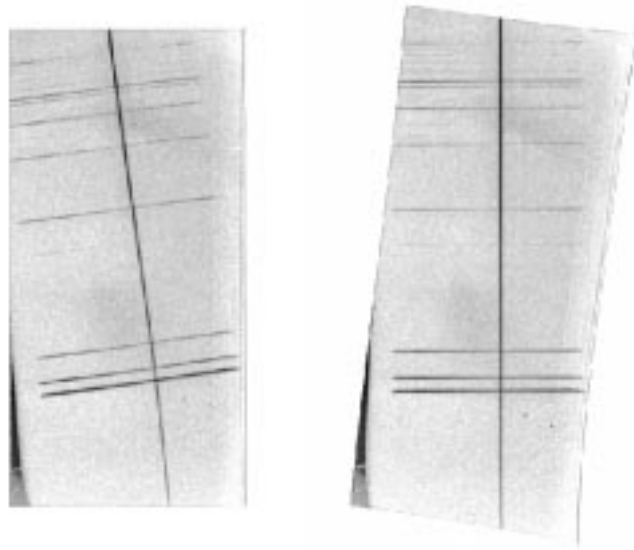


Figure 2. Result of the rectification process applied to calibration data. Left: Raw data, before geometric correction; Right: Rectified data

in the `noao.twodspec.longslit` package, the transformation between pixel position  $([i,j])$  and wavelength can be found.

In the perpendicular direction, along the slit, nature does not provide us with convenient linear arrangements of stars. The only way to overcome this is to take spectra of a single star at many different positions along the slit, an expensive proposition. In practice, a single star was positioned close to the center of the slit (to allow measurement of the trace of a star), and then moved approximately  $3''$  along the slit. The spectrum was geometrically rectified to make the central spectrum come out straight and vertical. The other spectrum was then examined to look for deviations from verticality. Any deviations show, to first order, that the scale along the slit is a function of wavelength. No significant deviations were found, so it was assumed that the same regularizing function can be applied to all positions along the slit.

Having created polynomial functions that convert from wavelength and position along the slit to pixel position  $[i, j]$ , we can create a reference file that, for each pixel in the rectified image, contains the coordinates of the corners of the quadrilateral that the pixel maps into in the raw data. Summing the contributions of the partial pixels covered by the quadrilateral (weighted by the intersection of the areas of raw pixels and mapped quadrilateral) gives the flux in the geometrically corrected pixel, calculated in a fashion that is rigorously flux-conserving. The HST Data Handbook gives an illustration of this process.

The result of geometrically correcting F/48 longslit data is shown in Figure 2, where a raw spectrum (actually the sum of a planetary nebula and a continuum point source) is shown before and after rectification.

This is all straightforward, but the time-dependence of the geometric distortion means that, in general, the reference files derived from calibration data are not quite applicable to science data. The error can amount to a few pixels at the extremes of the wavelength range, making any wavelength (or redshift) measurements incorrect at the few  $\text{\AA}$  (or few hundred km/s) level.

Since there is no facility to take calibration line spectra, the only monitor of the geometric distortion is the reseau marks. Most science images are not exposed enough to show the reseau marks, but fortunately all proposals were written to include internal flatfield

exposures during the occultation part of the orbit. Similarly, the calibration programs also included internal flatfield exposures to provide a snapshot of the geometric distortion at the time the calibration exposures were taken.

Using these internal flatfield exposures, it is relatively straightforward to create “custom” geometric correction reference files for each science exposure. We use the fact that the reseau marks have unique locations in the correctly geometrically corrected spectra (i.e., the geometrically corrected calibration spectra). The polynomial transformation applied to the reseau positions from the raw calibration flatfields gives the positions of the reseau marks in the geometrically corrected calibration images. Then all that is required is to determine the transformation required to go from the observed reseau mark positions in the flatfield appropriate to the science data to these reference reseau mark positions. There are tools in the `stsdas.hst_calib.foc.focgeom` package to assist in the locating of reseau marks (task `rfindx`) and fitting one set of reseau marks to another (task `rfitx`).

In practice, this method is relatively simple, convenient and robust. Typically, a  $5 \times 5$  polynomial fit with cross terms is required to give r.m.s residuals of the fit between raw and reference reseau positions of approximately 0.3 pixels. Generating reference files and geometrically correcting the data is then straightforward using the `p2geo` and `newgeom` tasks in the `focgeom` package.

It is possible to get small offsets between geometrically corrected spectra, both in the wavelength direction and in the direction along the slit. These can amount to a few pixels in each dimension, and is believed to be due to small differences in the way the spectrograph fold mirror is deployed from observation to observation. The difference is a pure shift, with no difference in dispersion or plate scale. Users should be aware of this possibility when combining multi-orbit observations.

The wavelength calibration and geometric rectification processes are described more fully in Voit (1997a, 1997b).

## 5. Spectrophotometric Calibration

The spectrophotometric calibration is performed by taking a spectrum of a spectrophotometric standard star. Comparison of the measured counts/second in the stellar spectrum with the known flux from the star gives the total sensitivity of the F/48 spectrograph in counts/( $\text{erg cm}^{-2} \text{ \AA}^{-1}$ ), or counts/photon.

Unfortunately, most of the spectrophotometric standard stars in the HST calibration reference library are too bright for the F/48 spectrograph to observe in first order without significant nonlinearity or saturation. Only the faintest standard star, LDS749B, is faint enough to be used in the linear regime. The reference spectrum uses the most recent corrections to the flux for both the UV spectrum (from IUE) and the visible (from Oke Double Spectrograph measurements), and is probably accurate to 10-20% or so in the UV and 5% or so in the visible.

Since we are trying to give an absolute calibration, it is very important to make sure that the star is accurately centered in the slit. An error of a few hundredths of an arcsecond in the centering can make a difference of more than 25% in the absolute calibration. For this reason, the calibration star was scanned across the slit in steps of  $0''.04$ , allowing a centering accuracy of  $0''.01$ – $0''.02$ . In practice, the spectrum with the highest throughput was sandwiched between two spectra with almost identical count rates, making interpolation of the maximum throughput straightforward.

Analysis of the point source profile along the slit direction shows that the FWHM is approximately 2 pixels, and that the slit transmits about 60% of the total flux of a point source if the flux along the slit is summed over a 10 pixel aperture. Conversion from measured flux to absolute flux depends on whether one is considering a point source or an extended source, and however the reference files are defined is sure to confuse some people.

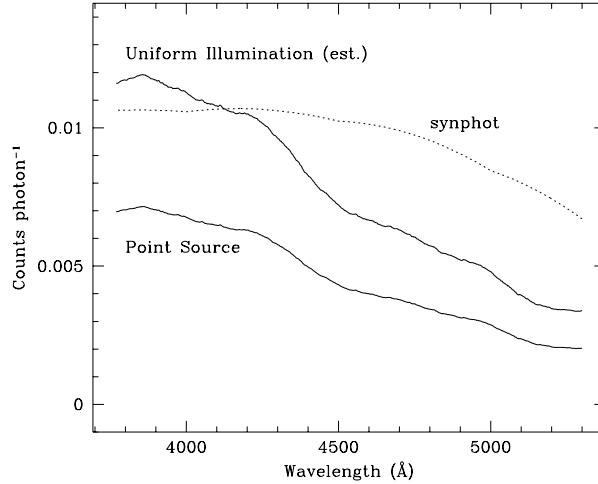


Figure 3. Spectrograph efficiency in counts/photon for first order spectra.

One could either keep all sensitivities in terms of “per pixel”, and advise users that when converting from measured fluxes to absolute fluxes for a point source, they should apply an aperture correction of  $1/0.6$  to account for the fact that only 60% of the flux from a point source passes through the slit. Alternatively, one could define the absolute sensitivity reference files to assume that point sources are observed, and advise users that when looking at an extended source, they should multiply the absolute calibrated fluxes by 0.6 to back out the aperture correction that is included in the reference files.

Comparison of the measured count rates with the known flux from the standard star gives the spectrograph efficiency curve shown in Figure 3. The two curves (for point and extended source) refer to the fact that the initial pre-launch calibration of the sensitivity of the spectrograph used an extended source. It can be seen that the sensitivity agrees with the pre-launch expectations reasonably well.

In a similar way, the sensitivity of the spectrograph in third order was measured by observing the same star with the F150W filter in place as an order extracting filter. This effectively cuts out all of the 1st and 2nd order flux and a large part of the fourth order flux, allowing a relatively clean measurement. The result of the sensitivity check is shown in Figure 4, where it is seen that the sensitivity agrees with the pre-launch estimates to within a factor of 2 over most of the wavelength region of interest.

Full details of the spectrophotometric calibration can be found in Voit & Jedrzejewski (1997).

## 6. Accuracies

If the rectification is performed using custom-generated references files, the absolute wavelength accuracy is limited by the repeatability of the deployment of the spectrograph mirror, to about 5 Å. However, relative wavelength measurements are much more accurate, amounting to approximately 0.5 pixels rms for both wavelength-to-wavelength comparisons and for comparisons at the same wavelength but different positions on the slit.

For spectrophotometry, the first-order accuracy is approximately 20% or so, while for third order the error is probably closer to 50%.

**Acknowledgments.** Richard Hook and Sperello di Serego Alighieri did some of the original work on the wavelength calibration of the F/48 spectrograph.

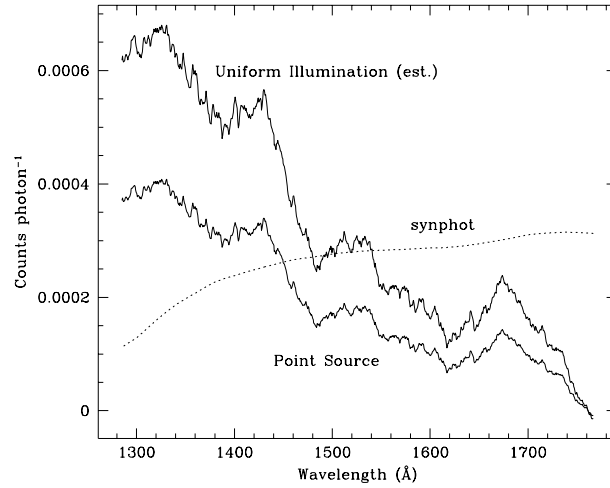


Figure 4. Spectrograph efficiency in third order

### References

- Voit, M., 1997a, Instrument Science Report FOC-96 (Baltimore: STScI)  
Voi, M., 1997b, Instrument Science Report FOC-97 (Baltimore: STScI)  
Voi, M., & Jedrzejewski, R., 1997, Instrument Science Report FOC-98 (Baltimore: STScI)